

## Article

# Disturbance of Wind Damage and Insect Outbreaks in the Old-Growth Forest of Changbai Mountain, Northeast China

Yuan Zhang <sup>1,2</sup>, Anzhi Wang <sup>1</sup>, Yage Liu <sup>1</sup>, Lidu Shen <sup>1</sup>, Rongrong Cai <sup>1</sup> and Jiabing Wu <sup>1,\*</sup>

<sup>1</sup> Key Laboratory of Forest Ecology and Management, Institute of Applied Ecology, Chinese Academy of Sciences, Shenyang 110016, China

<sup>2</sup> College of Resources and Environment, University of Chinese Academy of Sciences, Beijing 100049, China

\* Correspondence: wujb@iae.ac.cn

**Abstract:** The changing climate is worsening the threats to forests, such as insect outbreaks, fires, and drought, especially old-growth forest, which is more susceptible to disturbance. Therefore, it is important to detect the disturbance areas, identify the disturbance agents, and evaluate the disturbance intensity in old-growth forest. We tried to derive the forest disturbance information based on multiple remote sensing datasets (Global Forest Change, MODIS, and ERA5-Land) from 2000 to 2021 in Changbai Mountain, Northeast China, and explored their relationship with climate factors. The results showed that (1) wind damage and insect outbreaks are two main forest disturbance agents, (2) the increasing temperature during overwintering periods and the decreasing precipitation during activity periods increase the risk of insect outbreaks, and (3) disturbances lead to significant changes in forest structure and functional indices, which can be well captured by the remote sensing data. In the study, we creatively combined low-frequency remote sensing images and high-frequency meteorological data to determine the specific time of wind damage. The final results suggested that the vulnerability of old-growth forest to climate change may be mainly reflected through indirect implications, such as the increased risk of strong winds and insect disturbances.

**Keywords:** wind damage; insect outbreaks; old-growth forest; forest disturbance; larch caterpillar



**Citation:** Zhang, Y.; Wang, A.; Liu, Y.; Shen, L.; Cai, R.; Wu, J. Disturbance of Wind Damage and Insect Outbreaks in the Old-Growth Forest of Changbai Mountain, Northeast China. *Forests* **2023**, *14*, 368. <https://doi.org/10.3390/f14020368>

Academic Editor: Viacheslav I. Kharuk

Received: 5 January 2023

Revised: 2 February 2023

Accepted: 9 February 2023

Published: 12 February 2023



**Copyright:** © 2023 by the authors. Licensee MDPI, Basel, Switzerland. This article is an open access article distributed under the terms and conditions of the Creative Commons Attribution (CC BY) license (<https://creativecommons.org/licenses/by/4.0/>).

## 1. Introduction

Forests are among the most important ecosystems on earth, covering about 31% of the global land area [1]. Forest disturbance affects many ecological functions, including carbon storage, habitat value, and hydrological function. In the context of global changing, forest ecosystems have suffered serious disturbances that are driven prominently by warming [2]. Some disturbances, such as large-scale deforestation [3] and forest fires [4], which change dramatically and have clear boundaries, can easily be quantitatively assessed. However, some disturbances, such as wind damage and insect outbreaks, which are spatially discontinuous, are difficult to quantify and sometimes cannot even be recognized after being disturbed.

Climate change, especially warming, will expose forests to more risks. The rising temperatures will increase evaporation, which will increase the frequency of extreme precipitation events [5] and change storm systems [6]. Additionally, warming has increased the frequency of insect outbreaks. On the one hand, warming has led to an increase in continuous drought, which makes trees more vulnerable to pests and diseases; on the other hand, warming in winter increases the survival of overwintering insects, leading to frequent insect outbreaks. For example, warming showed a remarkable link with outbreaks, leading to higher insect outbreaks of five defoliating species in Center Europe [7]. In North American forests, climate change facilitated the mountain pine beetle's expansion into previously unsuitable habits [8]. Increasing dryness and active temperature promoted Siberian silk moth (*Dendrolimus sibiricus* Tschetv.) outbreaks, and shifted the outbreaks

boundary about 370 m uphill since 1950 [9]. A warming climate may improve food quality, provide better growth conditions for larval development [10], and increase the population growth and metabolic rates of insects [11], thus promoting more intense and frequent insect outbreaks.

Warming increases the frequency and intensity of extreme weather, especially extreme storms. Strong wind causes substantial defoliation, widespread snapping of trees, and even tree mortality. Intensified storm systems have brought more natural disasters to forests [12–16], as shown in studies focusing on satellite passive optical remote sensing of wind-induced forest damage, in which vegetation indices and algorithms are adopted to detect wind damage area and severity [15]. Compared with detection algorithms, proper selection of vegetation indices is more critical for obtaining satisfactory results [17]. The widely used indices consist of the normalized difference vegetation index (NDVI) [12,14], normalized difference infrared index (NDII) [13], enhanced vegetation index (EVI) [14,18], leaf area index (LAI), and fraction of photosynthetically active radiation (FPAR) [19]. After being disturbed by a strong wind, forests were damaged [14], all forest structure and functional indices, such as evapotranspiration (ET) declined [19], soil temperatures down to –50 cm increased [18], and the senescence in autumn accelerated, leading to a shorter growing season [16].

Old-growth forests are more sensitive to climate change, as well as other disturbances derived from climate change. Old-growth forest commonly has the characteristics of high tree species richness, old stand age, and vertical heterogeneity [20]. The capacity of old-growth forest to provide ecosystem services may be far more important to society than their use as a source of raw materials [21]. However, no old-growth stand will persist indefinitely. Old-growth forest degradation threatens biodiversity and the survival of species. Therefore, it is worth paying more attention to the disturbance processes of old-growth forest.

The National Natural Reserve of Changbai Mountain (NNR-CBM) was established in 1960, and it is one of the earliest nature reserves in China. No artificial damage is allowed in NNR-CBM; however, we observed forest biomass loss over the past 20 years. Thus, the objectives of this study were (I) to identify the forest disturbance area and agents in NNR-CBM, (II) to determine the influence of different forest disturbance agents through multiple indicators, and (III) to provide some suggestions for forest management and conservation.

## 2. Materials and Methods

### 2.1. Study Area

Our study area was located in the NNR-CBM in Jilin Province, Northeast China (Figure 1). The average annual temperature and precipitation of the whole area over the past 20 years were 4.7 °C and 686.6 mm, respectively. NNR-CBM is an old-growth mixed forest system, rich in tree species Korean pine (*Pinus koraiensis* Siebold et Zuccarini), *Larix olgensis* (*Larix olgensis* Henry), *Picea jezoensis* (*Picea jezoensis* Carr. var. *microsperma* (Lindl.) Cheng et L. K. Fu), etc. This area has a typical vertical forest gradient, including broad-leaved Korean pine mixed forest, spruce–fir forest, subalpine birch forest, and alpine tundra from low altitude to high altitude.

### 2.2. Data Source

Global Forest Change (GFC) v1.9 includes tree canopy cover for the year 2000 and forest loss from 2000 to 2021 at a spatial resolution of 30 m, which is based on Landsat 7 Enhanced Thematic Mapper Plus (ETM+) data [22]. The dataset quantifies global forest change using decision tree methodology. Comparable map and reference disturbance and gain results were achieved at the global and climate domain scales.

The Moderate Resolution Imaging Spectroradiometer (MODIS) instrument is operated on both Terra and Aqua spacecraft. Many data products derived from MODIS describe the biophysical features of the land (PTC: percentage tree cover, PNV: percentage nontree vegetation, NV: percentage non-vegetated, GPP: gross primary productivity, and LST: land

surface temperature), which can be used for the studies of processes and trends on global scales (Table 1).

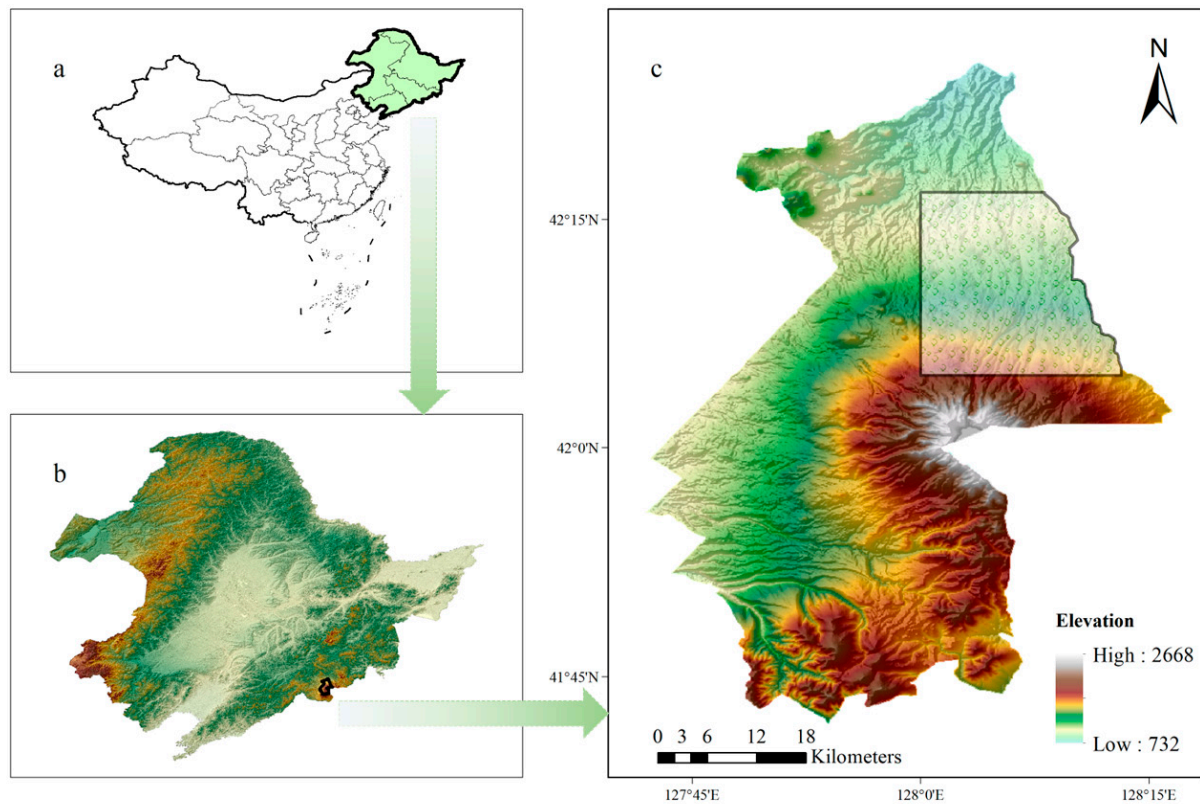


**Figure 1.** Geographical location of the study area in Northeast China. (a) Map of China. (b) Digital elevation model (DEM) shading map of Northeast China. (c) DEM shading map of the National Natural Reserve of Changbai Mountain, Northeast China. The black frame in (c) delineates the study area (459.56 km<sup>2</sup>).

**Table 1.** The specifications of the selected MODIS image products.

Biophysical Features	Products	Periods of Use	Spatial Resolution (m)	Temporal Resolution (Days)
PTC, PNV, and NV	MOD44B	2000–2020	250	365
NDVI	MOD13Q1	2015–2021	250	16
LAI	MCD15A3H	2015–2021	500	4
FPAR	MCD15A3H	2015–2021	500	4
GPP	MOD17A2H	2015–2021	500	8
ET	MOD16A2	2015–2021	500	8
LST	MOD11A2	2015–2021	1000	8

The land component of the fifth generation of European Reanalysis (ERA5-Land) is a reanalysis dataset describing the water and energy cycles with a grid spacing of 9 km and hourly temporal frequency [23]. The main meteorological variables include 2 m air temperature, wind speed, and total precipitation.

Google Earth Engine (GEE) combines a multi-petabyte catalog of satellite imagery and geospatial datasets. All the data mentioned above were processed and extracted using GEE.

Google Earth Pro (v7.3.6.9345, Google LLC., Milpitas, CA, USA) is a geospatial tool that provides historical imagery with high spatial resolution. Although the timelapse of the historical imagery is not fixed, these imageries can still provide some references for the change of the land.

### 2.3. Data Processing and Analysis

The procedure of the main method is illustrated in Figure 2. The first step was to identify the forest disturbance area and agents. The forest change of NNR was detected using the GFC dataset. Forest disturbance and the year of disturbance can be obtained from GFC. After the delineation of the forest disturbance area, through high-resolution images, field investigations, and a literature review, we determined the characteristics of forest disturbance agents.

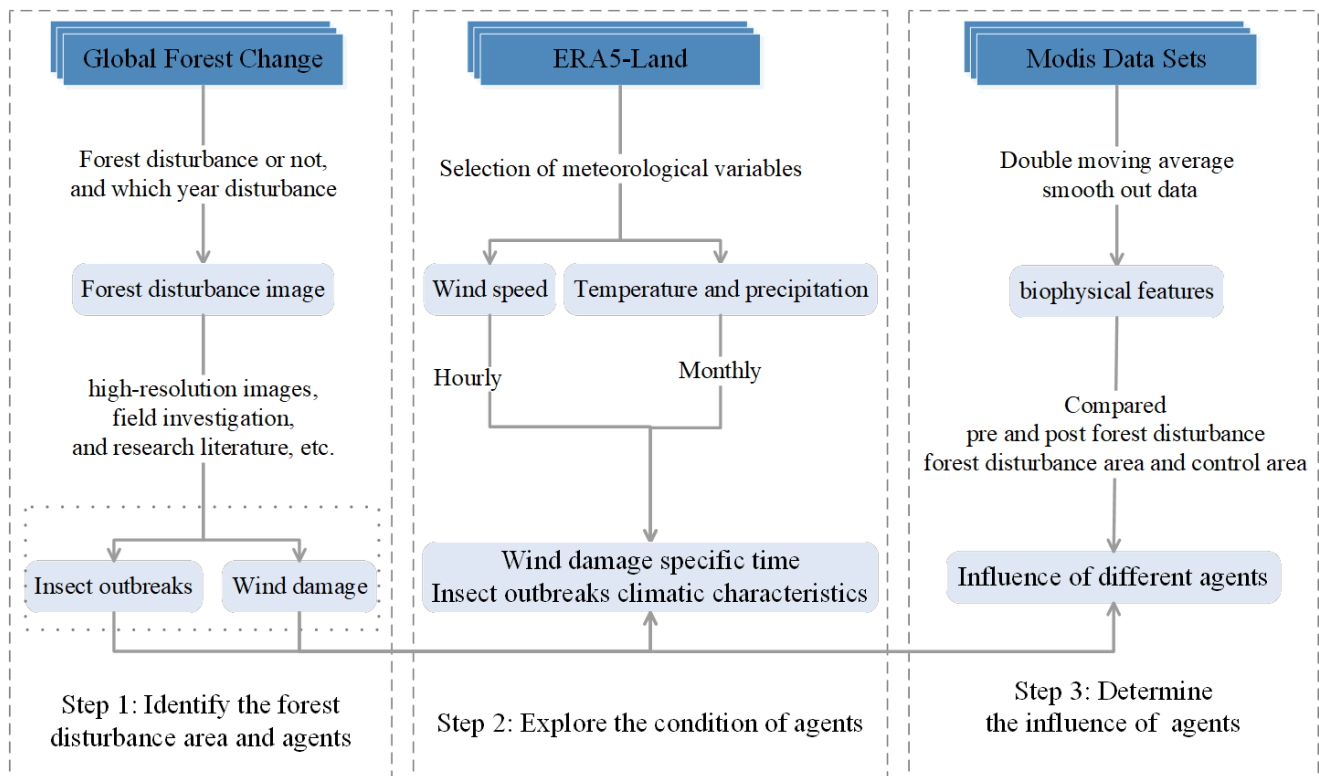


**Figure 2.** Flowchart describing the identification and influence of wind damage and insect outbreaks.

The second step was to explore the condition of agents. The wind speed characteristics in the wind damage area (WDA) and the climate characteristics in the insect outbreak area (IOA) were considered. These data were obtained from ERA5-Land. Wind speeds include both daily and hourly scales. High-temporal-resolution wind speed can help to determine the specific time of wind damage. Monthly air temperature and total precipitation can be better compared on an interannual scale.

The third step was to determine the influence of agents. Biophysical features were compared according to the agents of forest disturbance (WDA: wind damage area; IOA: insect outbreaks area). To better distinguish the effects of forest disturbance, we also compared the features of undisturbance areas (WDCA: wind damage control area; IOCA: insect outbreak control area) (Figure 3). These control areas were randomly selected from the area closed to corresponding agents.

Although the derived products of MODIS are composites, these products still have outliers. Double moving average (DMA) was used to help smooth out these data by creating constantly updated average data. The time window of DMA was 48 days. After DMA, the biophysical features could be better compared pre and post forest disturbance.

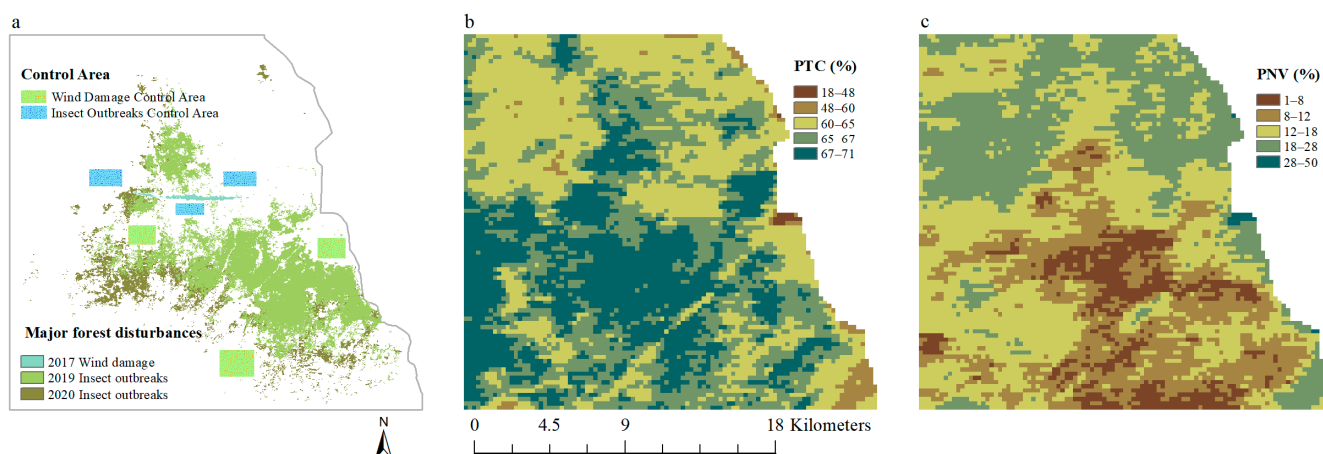


**Figure 3.** The major forest disturbances occurring in the National Natural Reserve of Changbai Mountain, Northeast China. The core area we defined exhibited drastic forest disturbance in the National Natural Reserve of Changbai Mountain. (a) Map of major forest disturbances and corresponding control area distribution. (b,c) Percentage tree cover (PTC) and percentage nontree vegetation (PNV), respectively.

### 3. Results

#### 3.1. Distribution of Forest Disturbance Areas

According to GFC data analysis, there were remarkable forest loss events from 2000 to 2021, mainly occurring in 2017, 2019, and 2020. These events mainly occurred in the core area (Figure 1). With the management of the Changbai Mountain Protection Development Management Committee, no deforestation and forest fires occurred in NNR-CBM. We inferred that these forest loss events may have been forest disturbances caused by wind damage or insect outbreaks. The corresponding shapes of the disturbance area were narrow linear, planar, or scattered distributions, respectively. We initially classified these disturbances into two major forest disturbances: wind damage and insect outbreaks, according to the shape of disturbance area.

The core area had high tree cover. The occurrence area and time of wind damage and insect outbreaks are shown in Figure 3a. The area of wind damage was 1.05 km<sup>2</sup>, and the altitude was about 1100 m. The length of the WDA was 5 km, and the width was 0.4 km, in the east–west direction. The IOA in 2019 and 2020 was 57.84 and 18.46 km<sup>2</sup>, respectively. The corresponding elevation was about 950–1450 m. The IOA showed an expanding tendency from 2019 to 2020.

#### 3.2. Wind Damage

From the GFC dataset, we can know that the narrow area lost its forest in 2017 (Figure 3). We finally identified the narrow area as WDA, according to the shape of the forest disturbance area, historical images (Figure 4), and field investigation.

The changes pre and post WDA were obvious from high-resolution images. The wind damage occurred between 3 May and 15 June 2017. To determine the exact time of occurrence, daily and hourly wind speed data (Figure 5) were taken into account. The wind speed at 7 a.m. on 7 May was maximal (hourly average wind speed, 8.32 m/s), reflecting 2.92 and 3.80 times the average annual wind speed in 2017 and past 20 years, respectively. We inferred that the wind damage occurred at this time.

The percentage tree cover of WDA changed rapidly in 2017 in the study area (Figure 6a), dropping from 67.74% to 41.20%. There was no significant change in the WDCA (Figure 6b). As PTC decreased, PNV increased, and NV did not change in WDA.

The changes in NDVI in WDA and WDCA were similar to the values pre wind damage. After being disturbed, extreme values (maximum and minimum) of NDVI in WDA were much lower than those in WDCA (Figure 7). This condition consistently lasted until the

fifth year (2021), for the restoration of vegetation. For LAI and FPAR, their remarkable changes in WDA were that the minimum region was lower than in WDCA. GPP was significantly lower in the wind damage year, and did not recover as NDVI did. The change in LST and ET was very small; the ET and LST trends decreased and increased, respectively.

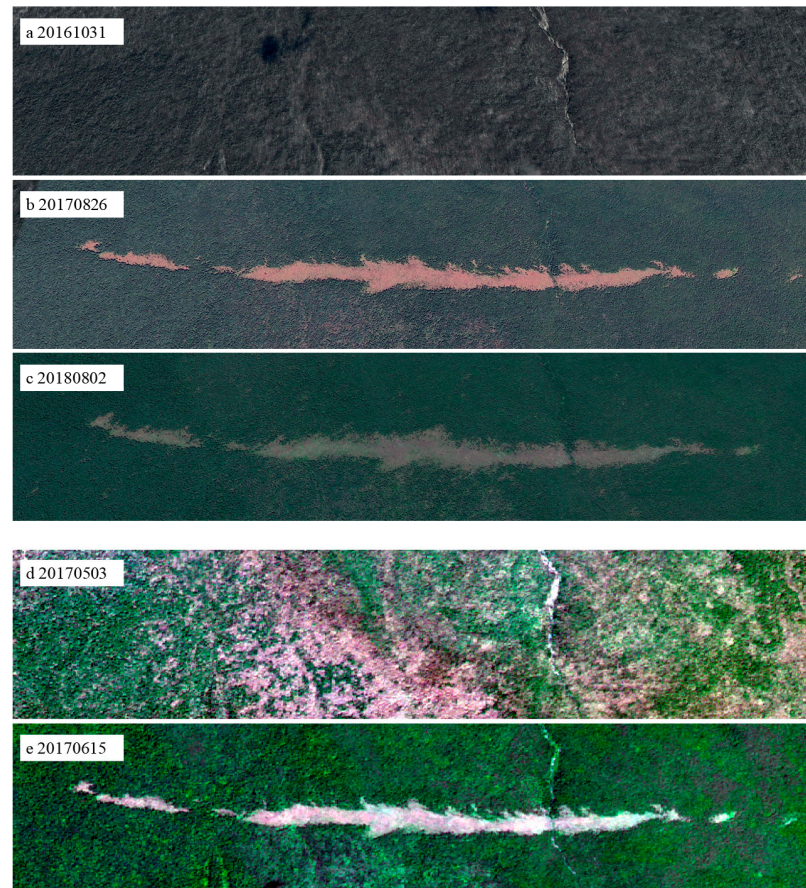


**Figure 4.** The images of the wind damage area. (a–c) Images acquired directly from Google Earth Pro. (d,e) True color RGB composites from the three bands of Sentinel-2 centered at 665, 560, and 490 nm. The numbers denote the corresponding times of the images (format: year/month/day).

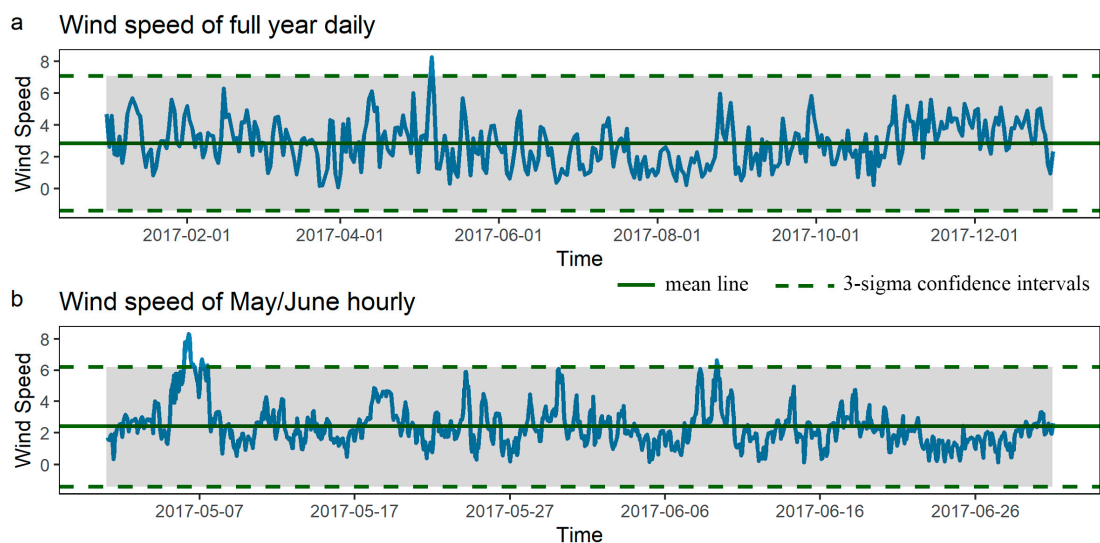


**Figure 5.** The daily (a) and hourly (b) wind speed data (m/s) of wind damage area in 2017. The shaded area denotes the confidence intervals of mean.

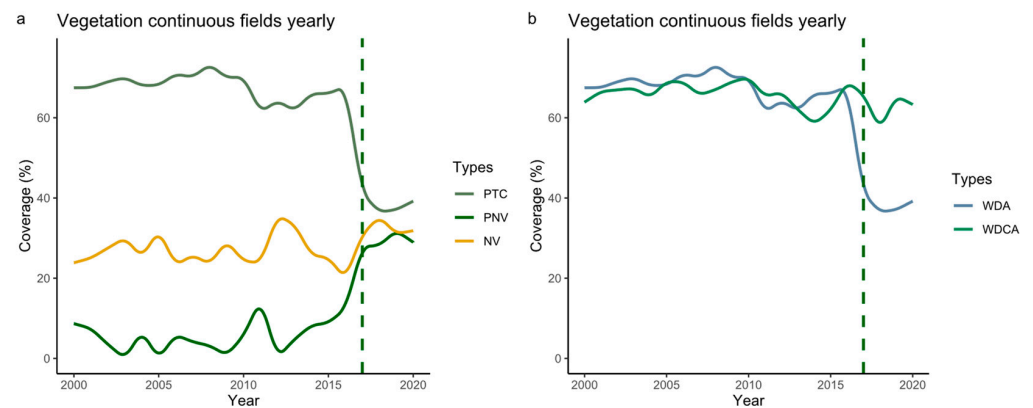


**Figure 6.** Percentage tree cover (PTC), percentage nontree vegetation (PNV), and percentage non-vegetated (NV) in wind damage area (WDA) (a); percentage tree cover of WDA and wind damage control area (WDCA) (b). The green dashed line denotes the year (2017) of wind damage.

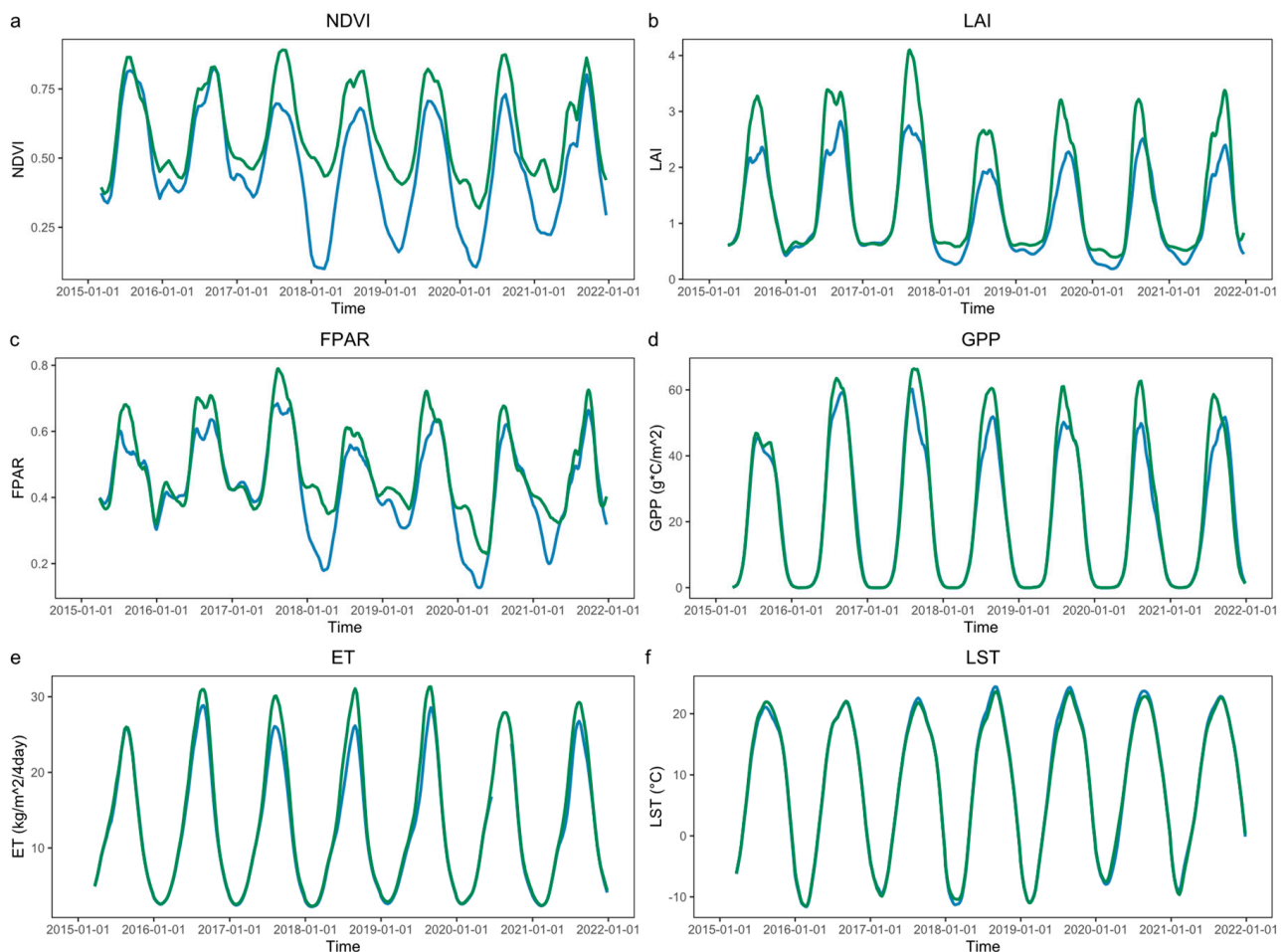


**Figure 7.** Biophysical features of wind damage area (blue solid line) and wind damage control area (green solid line). (a–f) are NDVI, LAI, FPAR, GPP, ET, and LST, respectively.

### 3.3. Insect Outbreaks

For the other forest disturbance area in Figure 3, considering the shape of the forest loss area, we initially ascribed it to large insect outbreak events. Field investigations and the literature review [24,25] further confirmed our assumption. The insect species is the larch caterpillar (*Dendrolimus superans* Butler), which is widely distributed in Eurasia [26]. *Larix olgensis* is regarded as the major host in spruce–fir forest. Their eggs are laid on

host needles, and developing larvae feed on host foliage. The larvae overwinter in the soil. In its native habitat region, the larch caterpillar usually takes 1 or 2 years to develop [27]. Mountain and hilly areas are more susceptible to pine caterpillar outbreaks [28]. We split the life history of the larch caterpillar [29] into two parts according to whether the larch caterpillar is in the tree or not, i.e., overwintering periods (October to the following March) and activity periods (April to September).

Comprehensive analysis suggested that the insect outbreaks started in 2019 and expanded in 2020. The PTC decreased rapidly from 63.79% to 53.09% to 44.10%, PVC increased rapidly from 14.97% to 19.90% to 27.90%, and the change in NV was not obvious from 2018 to 2020 in IOA. Meanwhile, in IOA-2020, the change in the three indicators was more extreme than in 2019 (Figure 8). PTC was even lower in IOA, compared to IOCA.

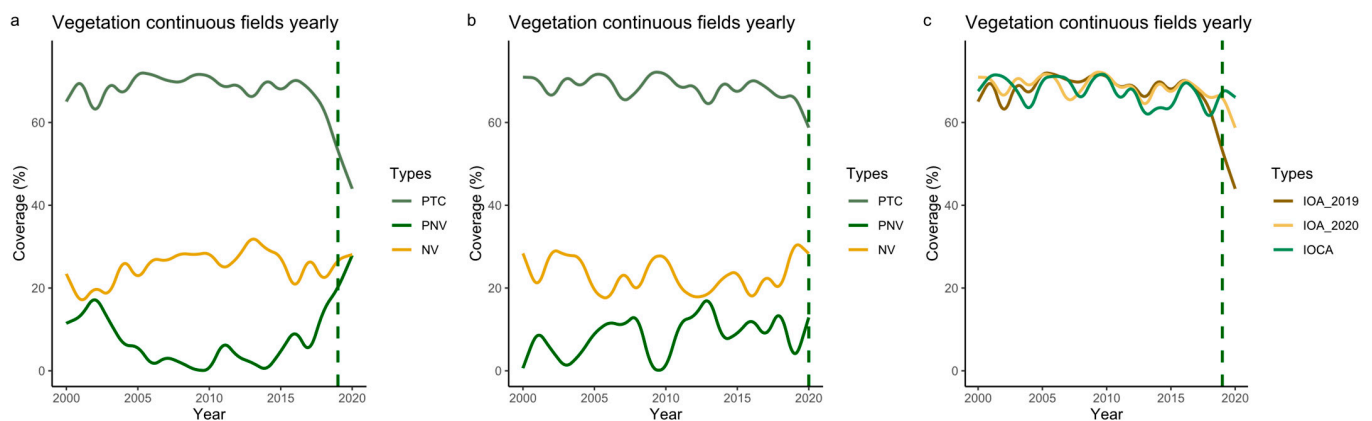


**Figure 8.** Percentage tree cover (PTC), percentage nontree vegetation (PNV), and percentage non-vegetated (NV) in insect outbreak area in 2019 (a) and 2020 (b); percentage tree cover in insect outbreak area in 2019 and 2020 (IOA\_2019, IOA\_2020) and insect outbreak control area (IOCA) (c). The green dashed line denotes the first year (2019) of insect outbreaks.

Forest susceptibility to caterpillar outbreaks was regulated by the interaction among topography, climate, soil, and forest type [28]. Some studies demonstrated that climatic warming and drying would increase the risk of larch caterpillar outbreaks, and suggested that increased precipitation had a very strong inhibitory effect on larch caterpillar outbreaks [29]. This is consistent with our results (Figure 9). The monthly maximum temperature, monthly average temperature, and monthly minimum temperatures during the overwintering periods were 2.7, 1.2, and 2.2 °C, respectively. All values were higher than the average in the winter before insect outbreaks, respectively. This provides the change for more larch caterpillars to survive the winter, which are ordinarily harsher and colder. At the same time, the precipitation decreased by 28.9% during activity periods, which allowed more caterpillars to ascend the tree and consume the foliage.

The changes in NDVI, LAI, and FPAR in the WDA and WDCA were similar pre insect outbreaks. Extreme values (maximum and minimum) of the WDA were lower than those of the WDCA (Figure 10). GPP was significantly lower in the insect outbreak year. The change in LST and ET was very small; the maximum ET and LST tended to decrease and increase, respectively.

Wind damage and insect outbreaks cause different intensities of forest disturbance and changes in biophysical features. Both led to decreases in PTC, NDVI, LAI, FPAR, GPP, and ET decrease, as well as increases in PNV and LST.

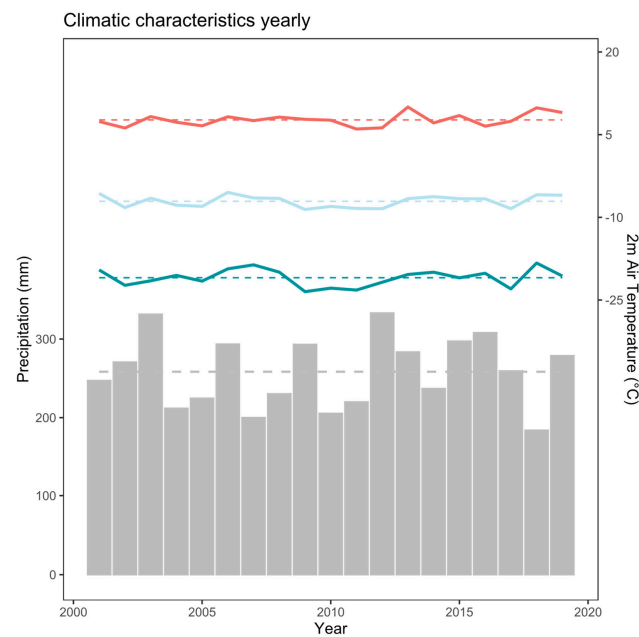


**Figure 9.** Climatic characteristics of insect outbreak area. The colorful broken line is the temperature during the overwintering periods. From top to bottom, the monthly maximum temperature, monthly average temperature, and monthly minimum temperature are shown; the colorful dashed line is the corresponding mean. The bars show the precipitation during activity periods, and the dashed line is the corresponding mean.

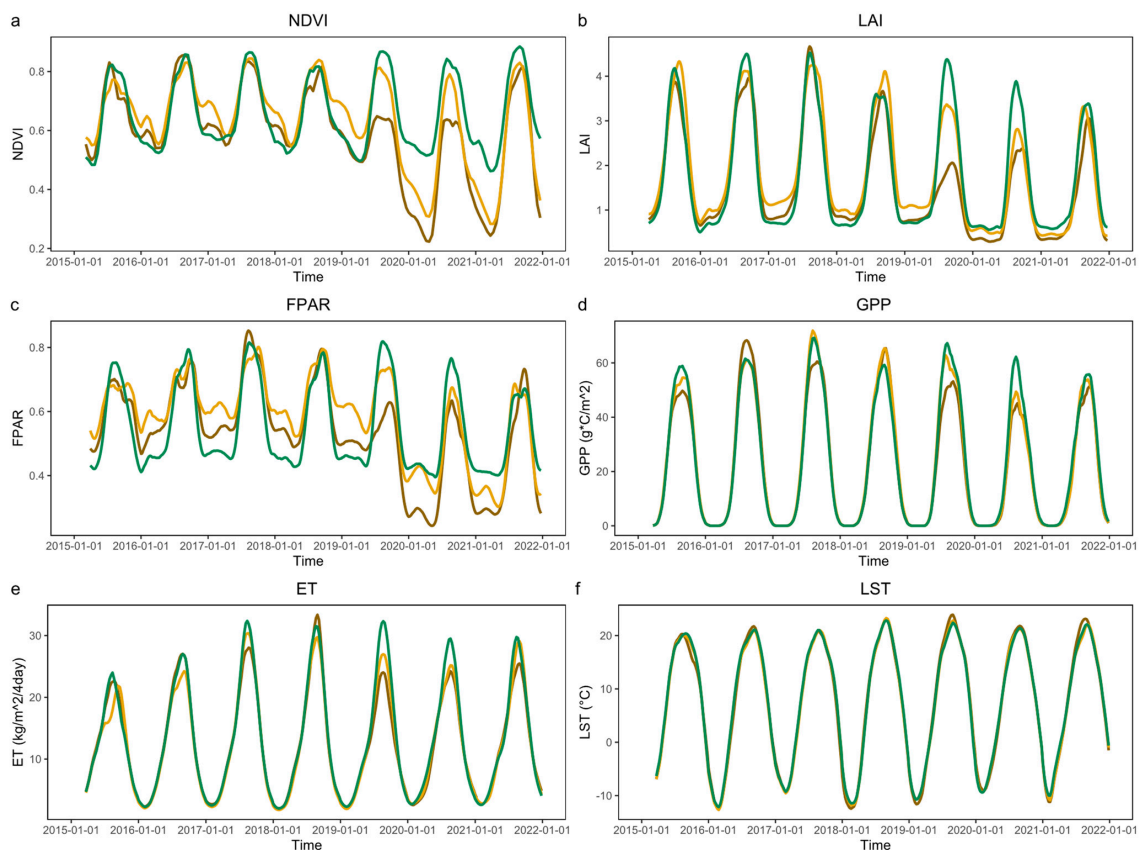


**Figure 10.** Biophysical features of insect outbreaks area (2019 and 2020) (deep-yellow solid line and pale-yellow solid line) and insect outbreak control area (green solid line). (a–f) are NDVI, LAI, FPAR, GPP, ET, and LST, respectively.

## 4. Discussion

### 4.1. The Phenology of the Region Changed after Forest Disturbance

As PTC decreased, PNV increased, whereas NV did not change in the WDA after wind damage (Figure 6). This indicates that the WDA was quickly occupied by other nontree vegetation that included communities of shrubs and grasses, similar to the changes in boreal larch forest after severe burn [30]. In a previous study, hurricanes accelerated autumn senescence by inducing an early end of the growing season and a shorter length of the growing season for the year of the storm [16]. This is consistent with our study. NDVI and GPP decreased more quickly in the fall after wind damage (Figure 7). We inferred this as due to the difference in phenology between trees and nontree vegetation.

The insect outbreaks not only caused the disturbance of NDVI, LAI, and FPAR [31], but also shortened the length of the growing season, similarly to wind damage. We inferred that the trees were more susceptible to being attacked by insects in spring than in other seasons. Both wind damage and insect outbreaks led to changes in regional phenology.

### 4.2. More Attention Should Be Paid to the Increase in Indirect Forest Disturbance Events Related to Climate Change

Studies on forest disturbance mainly focus on the forest disturbance area and the intensity of spatial disturbance caused by certain factors, such as deforestation and forest fires [14,15,28], whereas there is a lack of studies on disturbances with no remarkable space boundary transition, such as insect outbreaks. Our study creatively combined low-frequency remote sensing images and high-frequency meteorological data to determine the specific time of wind damage. This is crucial for forests that lack human management. Forest insect populations are influenced by temperature and other environmental conditions; thus, future changes in climate can be expected to affect forest insect outbreaks. Small-scale wind events are products of mesoscale climatic circumstances and, thus, may be affected by climate changes. These disturbances can create very large patches of damage. Windstorms can cause heavy mortality, produce canopy disruption, reduce tree density and size structure, and change local environmental conditions. The relationship between wind strength and the severity of disturbance is not constant across different forest types. For example, shallow-rooted species and thinned stands may be especially vulnerable to wind events. As a whole, more attention should be paid to the increase in indirect forest disturbance events related to climate change.

### 4.3. Enlightenment from Forest Disturbance events in Natural Forest Protection

Protection measures for natural forest protection are often extremely rigid, e.g., prohibiting any form of human intervention in the protected area. This measure brings about several achievements in natural forest protection, but may cause several problems as the tree age increases. For example, fuel loading is a key parameter in fire danger rating systems. In older-age forests, more and more fuel loading increases the fire risk. For mountain trees with umbrella-shaped roots, such as in our study area, older-age trees are more likely to fall in windy weather.

### 4.4. Some Limitations and Some Advice for Future Research

Passive optical remote sensing is one of the main methods for detecting forest disturbance, but it is easily affected by the weather. Few studies use active remote sensing [32] or multisource remote sensing. This is one possible future research direction.

We used remote sensing data to detect the disturbances of an old-growth forest in northeast China, which is a specific and unique region of the world; however, this method can be used more widely in other forest covered regions, for evaluating additional types of disturbances, such as forest fires and deforestation.

The WDA in our study area differs from areas damaged by tropical cyclones, typhoons, or hurricanes, which generally affect coastal areas. In inland China, especially Northeast China, typhoons are typically not a concern. However, the influence of local gusts under the

influence of cold air and cyclones on natural forests in Northeast China deserves attention, especially in mountain regions.

## 5. Conclusions

This study focused on the remote sensing detection of disturbances due to strong wind and insect outbreaks in an old-growth forest in Changbai Mountain, Northeast China. The results suggest that, under the background of global warming, more indirect disturbances may happen in old-growth forests. We could detect these disturbance agents and evaluate the forest restoration processes using multiple methods based on remote sensing data, as well as field investigations. The relevant detections and evaluations can be used as a reference for the study of forest disturbance, thus helping in the scientific management and protection of natural forests.

**Author Contributions:** Conceptualization, Y.Z. and A.W.; methodology, Y.Z.; validation, Y.Z., A.W. and J.W.; data curation, Y.Z.; writing—original draft preparation, Y.Z.; writing—review and editing, J.W., Y.L., L.S. and R.C.; visualization, Y.Z.; supervision, A.W.; funding acquisition, J.W. All authors have read and agreed to the published version of the manuscript.

**Funding:** This research was funded by the National Natural Science Foundation of China (32271873, 32171873, and 31971728).

**Institutional Review Board Statement:** Not applicable.

**Informed Consent Statement:** Not applicable.

**Data Availability Statement:** Publicly available datasets were analyzed in this study. These data can be obtained from the Google Earth Engine (<https://code.earthengine.google.com/> accessed on 6 February 2023).

**Conflicts of Interest:** The authors declare no conflict of interest.

## References

1. UNEP; FAO. *The State of the World's Forests 2020*; FAO: Rome, Italy, 2020. [CrossRef]
2. Seidl, R.; Thom, D.; Kautz, M.; Martin-Benito, D.; Peltoniemi, M.; Vacchiano, G.; Wild, J.; Ascoli, D.; Petr, M.; Honkaniemi, J.; et al. Forest disturbances under climate change. *Nat. Clim. Chang.* **2017**, *7*, 395–402. [CrossRef] [PubMed]
3. Diniz, C.G.; de Almeida Souza, A.A.; Santos, D.C.; Dias, M.C.; da Luz, N.C.; Vidal de Moraes, D.R.; Maia, J.S.A.; Gomes, A.R.; Narvaes, I.d.S.; Valeriano, D.M.; et al. DETER-B: The New Amazon Near Real-Time Deforestation Detection System. *Ieee J. Sel. Top. Appl. Earth Obs. Remote Sens.* **2015**, *8*, 3619–3628. [CrossRef]
4. Jiang, Y.; Zhou, L.; Raghavendra, A. Observed changes in fire patterns and possible drivers over Central Africa. *Environ. Res. Lett.* **2020**, *15*, 0940b8. [CrossRef]
5. Giorgi, F.; Raffaele, F.; Coppola, E. The response of precipitation characteristics to global warming from climate projections. *Earth Syst. Dyn.* **2019**, *10*, 73–89. [CrossRef]
6. Abell, J.T.; Winckler, G.; Anderson, R.F.; Herbert, T.D. Poleward and weakened westerlies during Pliocene warmth. *Nature* **2021**, *589*, 70. [CrossRef] [PubMed]
7. Silins, I.; Karklina, A.; Mieziute, O.; Jansons, A. Trends in Outbreaks of Defoliating Insects Highlight Growing Threats for Central European Forests, and Implications for Eastern Baltic Region. *Forests* **2021**, *12*, 799. [CrossRef]
8. Sidder, A.M.; Kumar, S.; Laituri, M.; Sibold, J.S. Using spatiotemporal correlative niche models for evaluating the effects of climate change on mountain pine beetle. *Ecosphere* **2016**, *7*, 22. [CrossRef]
9. Kharuk, V.I.; Im, S.T.; Soldatov, V.V. Siberian silkmoth outbreaks surpassed geoclimatic barrier in Siberian Mountains. *J. Mt. Sci.* **2020**, *17*, 1891–1900. [CrossRef]
10. Ren, P.; Neron, V.; Rossi, S.; Liang, E.; Bouchard, M.; Deslauriers, A. Warming counteracts defoliation-induced mismatch by increasing herbivore-plant phenological synchrony. *Glob. Chang. Biol.* **2020**, *26*, 2072–2080. [CrossRef]
11. Deutsch, C.A.; Tewksbury, J.J.; Tigchelaar, M.; Battisti, D.S.; Merrill, S.C.; Huey, R.B.; Naylor, R.L. Increase in crop losses to insect pests in a warming climate. *Science* **2018**, *361*, 916–919. [CrossRef]
12. Xu, S.; Zhu, X.L.; Helmer, E.H.; Tan, X.Y.; Tian, J.Q.; Chen, X.H. The damage of urban vegetation from super typhoon is associated with landscape factors: Evidence from Sentinel-2 imagery. *Int. J. Appl. Earth Obs. Geoinf.* **2021**, *104*, 102536. [CrossRef]
13. Zhang, X.; Chen, G.S.; Cai, L.X.; Jiao, H.B.; Hua, J.W.; Luo, X.F.; Wei, X.L. Impact Assessments of Typhoon Lekima on Forest Damages in Subtropical China Using Machine Learning Methods and Landsat 8 OLI Imagery. *Sustainability* **2021**, *13*, 4893. [CrossRef]

14. Mishra, M.; Kar, D.; Santos, C.A.G.; da Silva, R.M.; Das, P.P. Assessment of impacts to the sequence of the tropical cyclone Nisarga and monsoon events in shoreline changes and vegetation damage in the coastal zone of Maharashtra, India. *Mar. Pollut. Bull.* **2022**, *174*, 113262. [[CrossRef](#)] [[PubMed](#)]
15. Wang, W.T.; Qu, J.J.; Hao, X.J.; Liu, Y.Q.; Stanturf, J.A. Post-hurricane forest damage assessment using satellite remote sensing. *Agric. For. Meteorol.* **2010**, *150*, 122–132. [[CrossRef](#)]
16. Gong, Y.; Staudhammer, C.L.; Kenney, G.; Wiesner, S.; Zhang, Y.L.; Starr, G. Vegetation structure drives forest phenological recovery after hurricane. *Sci. Total Environ.* **2021**, *774*. [[CrossRef](#)]
17. Wang, F.G.; Xu, Y.J. Comparison of remote sensing change detection techniques for assessing hurricane damage to forests. *Environ. Monit. Assess.* **2010**, *162*, 311–326. [[CrossRef](#)]
18. Barr, J.G.; Engel, V.; Smith, T.J.; Fuentes, J.D. Hurricane disturbance and recovery of energy balance, CO<sub>2</sub> fluxes and canopy structure in a mangrove forest of the Florida Everglades. *Agric. For. Meteorol.* **2012**, *153*, 54–66. [[CrossRef](#)]
19. Bellanthudawa, B.K.A.; Chang, N.B. Hurricane Irma impact on biophysical and biochemical features of canopy vegetation in the Santa Fe River Basin, Florida. *Int. J. Appl. Earth Obs. Geoinf.* **2021**, *102*, 102427. [[CrossRef](#)]
20. Gutierrez, A.G.; Armesto, J.J.; Aravena, J.-C.; Carmona, M.; Carrasco, N.V.; Christie, D.A.; Pena, M.-P.; Perez, C.; Huth, A. Structural and environmental characterization of old-growth temperate rainforests of northern Chiloe Island, Chile: Regional and global relevance. *For. Ecol. Manag.* **2009**, *258*, 376–388. [[CrossRef](#)]
21. Hendrickson, O. Old-growth forests: Data gaps and challenges. *For. Chron.* **2003**, *79*, 645–651. [[CrossRef](#)]
22. Hansen, M.C.; Potapov, P.V.; Moore, R.; Hancher, M.; Turubanova, S.A.; Tyukavina, A.; Thau, D.; Stehman, S.V.; Goetz, S.J.; Loveland, T.R.; et al. High-Resolution Global Maps of 21st-Century Forest Cover Change. *Science* **2013**, *342*, 850–853. [[CrossRef](#)] [[PubMed](#)]
23. Muñoz Sabater, J. ERA5-Land hourly data from 1981 to present. Copernicus Climate Change Service (C3S) Climate Data Store (CDS). 2019. Available online: <https://cds.climate.copernicus.eu/cdsapp#!/dataset/10.24381/cds.e2161bac?tab=overview> (accessed on 1 October 2022).
24. Yu, D.; Zheng, Y.; Zhang, L.-j.; Sun, C.; Li, J.; Zhao, C.; Liu, L. Investigation and Factors Analysis of *Dendrolimus superans* Outbreaks in Changbai Mountain National Nature Reserve. *For. Res.* **2022**, *35*, 103–111. [[CrossRef](#)]
25. Zhao, C.; Xu, J.; Sun, C.; Jin, Y.; Shui, X.; Tao, Y.; Zhang, H.; Zhang, Y.; Liu, L. Analysis of meteorological factors for outbreak of Larch caterpillar in Changbai Mountains under the background of climate change. *J. Northeast Norm. Univ. (Nat. Sci. Ed.)* **2022**, *54*, 141–149. [[CrossRef](#)]
26. Zeng, J.; Feng, G.; Su, J.; He, Z. Researches on the occurrences of major forest insect pests of pine caterpillar *Dendrolimus* spp. in China. *Chin. Bull. Entomol.* **2010**, *47*, 451–459.
27. Bragard, C.; Baptista, P.; Chatzivassiliou, E.; Di Serio, F.; Gonthier, P.; Jaques Miret, J.A.; Justesen, A.F.; Magnusson, C.S.; Milonas, P.; Navas-Cortes, J.A.; et al. Pest categorisation of *Dendrolimus superans*. *EFSA J. Eur. Food Saf. Auth.* **2022**, *20*, e07525. [[CrossRef](#)]
28. Bao, Y.; Han, A.; Zhang, J.; Liu, X.; Tong, Z.; Bao, Y. Contribution of the synergistic interaction between topography and climate variables to pine caterpillar (*Dendrolimus* spp.) outbreaks in Shandong Province, China. *Agric. For. Meteorol.* **2022**, *322*, 109023. [[CrossRef](#)]
29. Fang, L.; Yu, Y.; Fang, G.; Zhang, X.; Yu, Z.; Zhang, X.; Crocker, E.; Yang, J. Effects of meteorological factors on the defoliation dynamics of the larch caterpillar (*Dendrolimus superans* Butler) in the Great Xing'an boreal forests. *J. For. Res.* **2021**, *32*, 2683–2697. [[CrossRef](#)]
30. Chu, T.; Guo, X.; Takeda, K. Effects of Burn Severity and Environmental Conditions on Post-Fire Regeneration in Siberian Larch Forest. *Forests* **2017**, *8*, 76. [[CrossRef](#)]
31. Huang, L.; Ning, Z.Y.; Zhang, X.L. Impacts of caterpillar disturbance on forest net primary production estimation in China. *Ecol. Indic.* **2010**, *10*, 1144–1151. [[CrossRef](#)]
32. Tanase, M.A.; Aponte, C.; Mermoz, S.; Bouvet, A.; Toan, T.L.; Heurich, M. Detection of windthrows and insect outbreaks by L-band SAR: A case study in the Bavarian Forest National Park. *Remote Sens. Environ.* **2018**, *209*, 700–711. [[CrossRef](#)]

**Disclaimer/Publisher's Note:** The statements, opinions and data contained in all publications are solely those of the individual author(s) and contributor(s) and not of MDPI and/or the editor(s). MDPI and/or the editor(s) disclaim responsibility for any injury to people or property resulting from any ideas, methods, instructions or products referred to in the content.